ACCEPTED FOR PUBLICATION IN THE 10 SEPTEMBER 2004 EDITION OF APJ
Preprint typeset using LaTeX style emulateapj v. 4/9/03

FAR ULTRAVIOLET OBSERVATIONS OF MOLECULAR HYDROGEN IN THE DIFFUSE INTERSTELLAR MEDIUM OF STARBURST GALAXIES[1]

CHARLES G. HOOPES[2], KENNETH R. SEMBACH[3], TIMOTHY M. HECKMAN[2], GERHARDT R. MEURER[2], ALESSANDRA ALOISI[3,4], DANIELA CALZETTI[3], CLAUS LEITHERER[3], & CRYSTAL L. MARTIN[5]

Draft version February 2, 2008

ABSTRACT

The 905 to 1180 Å spectral range of the *Far Ultraviolet Spectroscopic Explorer* (*FUSE*) includes numerous transitions of molecular hydrogen, making it possible to study H_2 in diffuse interstellar environments directly through absorption measurements. We have searched for H_2 absorption in five starburst galaxies: NGC 1705, NGC 3310, NGC 4214, M83 (NGC 5236), and NGC 5253. We tentatively detect weak absorption by H_2 in M83 and NGC 5253, and set upper limits on the H_2 column density in the other galaxies. Conservative upper limits on the mass of molecular gas detected with *FUSE* are many orders of magnitude lower than the H_2 mass inferred from CO emission measurements for the four galaxies in our sample in which CO has been detected. This indicates that almost all of the H_2 is in the form of clouds with $N(H_2) \gtrsim 10^{20}$ cm^{-2} that are opaque to far-UV light and therefore cannot be probed with far-UV absorption measurements. The far-UV continuum visible in the *FUSE* spectra passes between the dense clouds, which have a covering factor < 1. The complex observational biases related to varying extinction across the extended UV emission in the *FUSE* apertures prevent an unambiguous characterization of the diffuse H_2 in these starbursts. However, the evidence is suggestive that there is less H_2 in the diffuse interstellar medium between the dense clouds compared to similarly reddened sight lines in the Milky Way. This holds with the expectation that the destructive UV radiation field is stronger in starbursts. However, previous UV observations of these starbursts have shown that there is reddening caused by the diffuse interstellar medium. This suggests that while diffuse H_2 may be destroyed in the starburst, dust still exists.

Subject headings: galaxies: starburst — galaxies: individual (NGC 1705, NGC 3310, NGC 4214, NGC 5236 (M83), NGC 5253) — ultraviolet: ISM — ISM: molecules

1. INTRODUCTION

The complex interaction between gas and stars exists in all star-forming galaxies, but can perhaps be most easily studied in the extreme conditions of starbursts. The high rate of star formation in these galaxies implies that the gravitational collapse of molecular clouds is proceeding at a pace much greater than that seen in normal galaxies. Once star formation has begun, the remaining gas is exposed to the destructive UV radiation field emitted by the most massive new stars. Illuminating the details of this relationship is a crucial step toward understanding the evolution of galaxies through time.

Molecular hydrogen is the fuel for star formation, so it is natural to expect large amounts of H_2 to exist in starburst regions. Indeed, mm-wave observations using CO as a tracer of H_2 imply the presence of $\sim 3 \times 10^8$ $M_\odot$ of molecular gas in the starburst region of M82 (Weiss et al. 2001). However, observations of some starbursts reveal little or no CO emission, such as NGC 1705 (Greve et al. 1996) and I Zw 18 (*e.g.*, Gondhalekar et al. 1998). The lack of CO detections is difficult to interpret for metal-poor galaxies because the CO to H_2 conversion is metallicity-dependent (Wilson 1995).

It is possible to study H_2 *directly* using far-UV spectroscopy. There are numerous transitions of molecular hydrogen in the far-UV, allowing the direct measurement of H_2 and eliminating the uncertainty caused by the conversion from CO. Furthermore, far-UV absorption studies can probe H_2 in column densities much lower than can be studied through CO line emission, making it possible to study H_2 in the diffuse ISM. CO studies typically detect molecular gas with H_2 column densities in the range of 10^{20} to 10^{23} cm^{-2}, while absorption studies have probed lines of sight in the Milky Way and Magellanic Clouds with H_2 column densities from 10^{14} to 10^{21} cm^{-2} (Savage et al. 1977; Dixon, Hurwitz, & Bowyer 1998; Tumlinson et al. 2002). However, unlike radio observations, far-UV measurements are profoundly affected by extinction. In particular, absorption measurements toward extended continuum sources with inhomogeneous extinction can be very difficult to interpret (*e.g.*, Bluhm et al. 2003). Such observations must be treated carefully in order to derive correct conclusions about the H_2 content of galaxies.

Far-UV absorption studies have shown that H_2 is common in the diffuse ISM when the shielding along the sight line is sufficient to prevent dissociation by the interstellar UV radiation field. In the Milky Way, the transition occurs at $E(B-V) \sim 0.08$, and sight lines with at least this much reddening almost always contain H_2 (Savage et al. 1977). Investigation of the relationship between $N(H_2)$ and $E(B-V)$ in environments that differ from the Milky Way, such as the intense radiation environment of starbursts, can shed light on the formation and destruction mechanisms for H_2 and dust. Previous *FUSE* investigations of H_2 absorption in metal-poor

[1] Based on observations made with the NASA-CNES-CSA Far Ultraviolet Spectroscopic Explorer. FUSE is operated for NASA by the Johns Hopkins University under NASA contract NAS5-32985.

[2] Department of Physics and Astronomy, Johns Hopkins University, 3400 N. Charles St., Baltimore, MD 21218; choopes@pha.jhu.edu, heckman@pha.jhu.edu, meurer@pha.jhu.edu

[3] Space Telescope Science Institute, 3700 San Martin Dr., Baltimore, MD 21218; sembach@stsci.edu, aloisi@stsci.edu, calzetti@stsci.edu, leitherer@stsci.edu

[4] On assignment from the Space Telescope Division of ESA. Previous address: Department of Physics and Astronomy, Johns Hopkins University, 3400 N. Charles St., Baltimore, MD 21218

[5] Department of Physics, University of California at Santa Barbara, Santa Barbara, CA 93106; cmartin@physics.ucsb.edu

TABLE 1. PROPERTIES OF THE STARBURST GALAXIES IN THE SAMPLE

Galaxy	Type[a]	Distance[b] (Mpc)	Radial Velocity[c] (km s^{-1})	12+log(O/H)[d]	E(B-V)[e]
NGC 1705	Irr AM	5.1	569	8.0	0.0
NGC 3310	SAB(r)bc	14.5	1018	9.0	0.3
NGC 4214	IAB(s)m	2.9	298	8.2	0.2
M83(NGC 5236)	SBc	4.5	503	9.3	0.3
NGC 5253	Im Am	3.3	416	8.2	0.2

[a]Galaxy Hubble types were taken from Kinney et al. 1993

[b]References for distances are: Tosi et al. 2001 for NGC 1705, Maíz-Apellániz, Cieza, & MacKenty 2002 for NGC 4214, Thim et al. 2003 for M83, and Gibson et al. 2000 for NGC 5253. The distance to NGC 3310 was derived assuming H_0 = 70 km s^{-1} Mpc^{-1}

[c]Radial velocities were taken from de Vaucouleurs et al. 1991 except NGC 1705, which was taken from Heckman et al. 2001a.

[d]Abundances in the inner H II regions. References for 12+log(O/H) values are taken from the compilation in Heckman et al. (1998).

[e]The estimated intrinsic reddening (excluding the foreground Milky Way). These are based on the measurements of the far-UV spectral energy distribution (Meurer, Heckman, & Calzetti 1999; Leitherer et al. 2002), and the Calzetti (2001) effective starburst attenuation law.

starbursts have set low upper limits on the amount of H_2 in the diffuse ISM (Vidal-Madjar et al. 2000; Thuan, Lecavelier des Etangs, & Izotov 2002; Aloisi et al. 2003), and since these galaxies have not been detected in CO it is possible that they contain very little H_2 in denser environments as well. It is not clear whether the low metal content or the starburst radiation environment is responsible for the lack of H_2. To fully understand the behavior of H_2 in the diffuse ISM of starbursts, the sample must be extended to galaxies with higher metal content and to those in which CO emission has been detected.

We have used the *Far Ultraviolet Spectroscopic Explorer* (*FUSE*; Moos et al. 2000) to search for H_2 absorption in five starburst galaxies: NGC 1705, NGC 3310, NGC 4214, M83 (NGC 5236), and NGC 5253. The properties of these galaxies are given in Table 1. Four of these galaxies have been detected in CO emission, while NGC 1705 has not. The *FUSE* observations use the OB stars in the starburst as the UV continuum source, and probe absorption by gas in front of the starburst. The *FUSE* spectra show surprisingly little absorption from H_2 in the diffuse ISM, which may be a result of observational selection effects, but may also indicate the H_2 is destroyed in starbursts.

2. OBSERVATIONS AND DATA REDUCTION

A log of the *FUSE* observations is given in Table 2, and more information can be found in Heckman et al. (2001b). The *FUSE* mission and instrument are described by Moos et al. (2000) and Sahnow et al. (2000). The spectra were obtained through the LWRS ($30'' \times 30''$) apertures except for NGC 5253, which was observed through the MDRS ($4'' \times 20''$) apertures. Figures 1 – 5 show the location of the *FUSE* apertures for each galaxy.

The raw spectra were processed through the *FUSE* calibration pipeline (CALFUSE v2.1.6). The pipeline screens data for passage through the South Atlantic Anomaly and low Earth limb angle pointings and corrects for thermal drift of the gratings, thermally-induced changes in the detector readout circuitry, and Doppler shifts due to the orbital motion of the satellite. Finally, the pipeline subtracts a constant detector background and applies wavelength and flux calibration. After the pipeline reduction the individual spectra were co-added to produce the final calibrated spectrum.

FUSE consists of 4 co-aligned optical channels, two optimized for longer wavelength (LiF1 and LiF2; 1000 – 1187 Å) and two optimized for shorter wavelengths (SiC1 and SiC2; 905 – 1100 Å). The data from the four channels were analyzed separately, because there are slight differences in the spectral resolution between channels which can cause problems if the channels are co-added. Treating the channels separately also provides a safeguard against detector defects. The velocity zero-point of each individual channel was found using strong Galactic absorption lines.

3. NOTES ON THE INDIVIDUAL GALAXIES

Several of the starbursts are essentially point sources in the far-UV, and the interpretation of their spectra is fairly simple. Others, however, are extended far-UV sources with varying extinction. In these sources the morphology and extinction must be taken into account in order to understand the information in the *FUSE* spectra. In this section we describe the far-UV morphology of each galaxy and how it may affect the results. We also review previous results of CO emission measurements, in order to contrast them with the UV absorption measurements presented in the next section.

NGC 1705: The strongest far-UV source in NGC 1705 is the central star cluster NGC 1705-1, although there is a significant contribution from other far-UV sources (Meurer et al. 1995). The galaxy is small enough that the entire UV-emitting region fits within the *FUSE* LWRS aperture. Figure 1 shows an archival *Hubble Space Telescope (HST)* WFPC2 U-band (F380W) image and an archival FOC image (F220W). The bright point-like nature of NGC 1705-1 is illustrated by the point spread function apparent in the pre-costar FOC image. NGC 1705 is metal-poor (Meurer et al. 1992; Storchi-Bergmann, Calzetti, & Kinney 1994; Heckman et al. 1998, 2001a) and has not been detected in CO (Greve et al. 1996).

NGC 3310: Figure 2 shows an *Ultraviolet Imaging Telescope (UIT)* far-UV (B1 filter: 1520 Å) image of NGC 3310, and a FOC near-UV image (F220W) of the central region. The image shows that most of the star-forming regions in this galaxy fit within the LWRS aperture. A UV-bright core is surrounded by a star-forming ring. Conselice et al. (2000) showed that the nucleus is actually quite red compared to the ring, indicating that it is either very dusty or is dominated by older stars. Using the UIT image shown in Figure 2, Smith et al. (1996) concluded that the nucleus is heavily extinguished in the far-UV, and that the starburst ring is the strongest far-UV source. The far-UV light in the *FUSE* spectrum is a composite of all of these star-forming regions, but it is weighted toward the bluer regions in the ring and the

TABLE 2. LOG OF OBSERVATIONS

Galaxy	Data Set ID	Observation Date	T_{exp} (ks)	Aperture
NGC 1705	A0460102,A0460103	2000 Feb 4-5	21.3	$30'' \times 30''$
NGC 3310	A0460201	2000 May 5	27.1	$30'' \times 30''$
NGC 4214	A0460303	2000 May 12	20.7	$30'' \times 30''$
M83 (NGC 5236)	A0460505	2000 Jul 6	26.5	$30'' \times 30''$
NGC 5253	A0460404	2000 Aug 7	27.4	$4'' \times 20''$

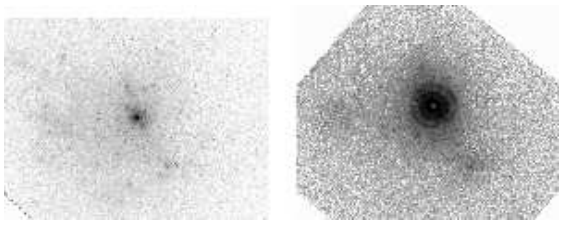

FIG. 1.— Ultraviolet images of NGC 1705. *Left:* An archival WFPC2 U-band (F380W) image. This image is approximately $21'' \times 17''$, so everything in the image falls within the LWRS aperture. *Right:* An archival FOC near-UV (F220W) image. The galaxy is essentially a point source in the UV, so the pre-costar point spread function of *HST* is apparent. North is up and East is left in both images.

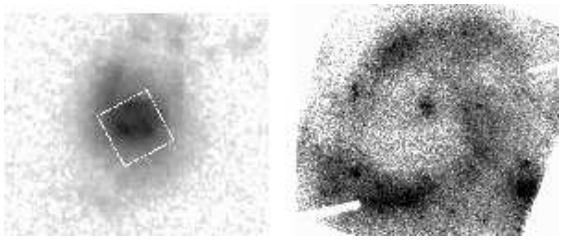

FIG. 2.— Ultraviolet images of NGC 3310. *Left:* A UIT 1520 Å (B1) image (Smith et al. 1996), showing the location of the *FUSE* $30'' \times 30''$ LWRS aperture. *Right:* An archival FOC near-UV (F220W) image of the starburst region. The image is approximately $28'' \times 24''$. The LWRS aperture is centered south of the nucleus, at approximately the position of the star-forming ring. North is up and East is left in both images.

UV-bright knot in the southwest (known as the "jumbo" H II region, Balick & Heckman 1981). There is molecular gas traced by CO in this knot, but the highest concentration of CO is in the northwest part of the ring (Kikumoto et al. 1993). Mulder et al. (1995) found $\sim 10^8$ $M_\odot$ of H_2, most of which is located within the region probed by the *FUSE* pointing.

NGC 4214: The left panel of Figure 3 is a *UIT* far-UV image of NGC 4214, with the *FUSE* LWRS aperture located on the central starburst (NGC 4214-I). The right panel shows an archival WFPC2 far-UV (F170W) image of the central region. The strongest far-UV emission comes from NGC 4214-I, so the *FUSE* spectrum is essentially a spectrum of this cluster. This source lies in an extended component of diffuse CO emission, containing $\sim 8 \times 10^5$ $M_\odot$ of H_2 (Walter et al. 2001), and is in a "hole" in the Hα emission (Leitherer et al. 1996).

M83 (NGC 5236): The left panel of Figure 4 is a UIT far-UV (1520 Å) image of M83, with the *FUSE* LWRS aperture located on the central starburst. The right panel shows an archival WFPC2 U-band (F300W) image of the central region. Harris et al. (2001) used this image to show that the central region contains at least 39 star clusters less than 10 Myr old. These clusters should have strong far-UV emis-

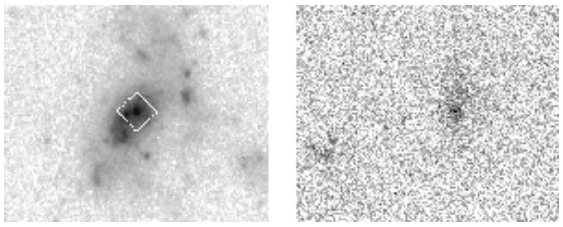

FIG. 3.— Ultraviolet images of NGC 4214. *Left:* A UIT 1520 Å (B1) image, showing the location of the *FUSE* $30'' \times 30''$ LWRS aperture. *Right:* A WFPC2 far-UV (F170W) image of the starburst region. The image is approximately $21'' \times 17''$, so everything in the image falls within the LWRS aperture. North is up and East is left in both images.

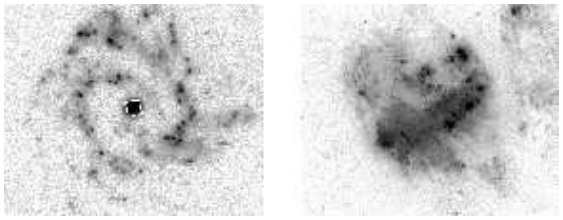

FIG. 4.— Ultraviolet images of M83. *Left:* A UIT 1520 Å (B1) image, showing the location of the *FUSE* $30'' \times 30''$ LWRS aperture. *Right:* A WFPC2 U-band (F300W) image of the starburst region of M83. The image is approximately $21'' \times 17''$, so everything in the image falls within the LWRS aperture. North is up and East is left in both images.

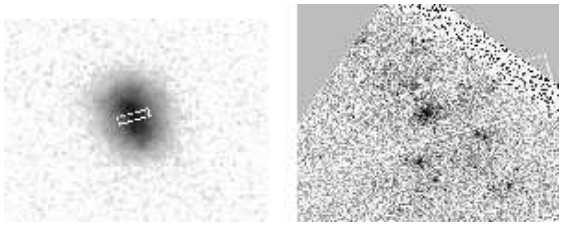

FIG. 5.— Ultraviolet images of NGC 5253. *Left:* A UIT 1520 Å (B1) image, showing the location of the *FUSE* $4'' \times 20''$ MDRS aperture. *Right:* A WFPC2 far-UV (F170W) image, also showing the location of the *FUSE* MDRS aperture. North is up and East is left in both images.

sion, so the *FUSE* spectrum is a combination of many individual sight lines. Israel et al. (2001) found that the central region (roughly coincident with the LWRS aperture) contains $\sim 10^7$ $M_\odot$ of H_2 from observations of CO emission.

NGC 5253: This is the only galaxy for which the MDRS aperture was used. Figure 5 shows the placement of the aperture on a UIT far-UV image and an archival WFPC2 far-UV image. The region observed includes the brightest cluster in the far-UV (Meurer et al. 1995), but no other regions of significant star formation. Meier, Turner, & Beck (2002) found that this region contains $\sim 10^5$ $M_\odot$ of H_2 from obser-

vations of CO emission. Soft X-ray emission is associated with the cluster, suggesting the presence of a superbubble (Strickland & Stevens 1999).

4. COLUMN DENSITY MEASUREMENTS

4.1. *Molecular Hydrogen*

Absorption profiles for each galaxy are shown in Figure 6. Each panel in the figure shows the Si II 1020.699 Å absorption profile (which traces the neutral ISM) as well as one H_2 absorption profile for each rotation level from $J = 0-4$ (except for NGC 3310, for which no suitable $J = 4$ line was found). The lines shown were chosen because they are the strongest lines that are not blended with any other absorption, either intrinsic or Galactic. Absorption from H_2 is only visible in the $J = 1$ and $J = 2$ levels in NGC 5253 and in the $J = 1$ level of M83. The NGC 5253 detections in the LiF1 spectrum are both $\sim 3\sigma$ or better, but the absorption is not obvious in the less-sensitive LiF2 channel, so the detections in LiF1 are tentative. There is also a possible detection in the $J = 3$ level for NGC 5253, but this would be at $< 2\sigma$ significance and is not confirmed in the LiF2 spectrum so we do not count it as a detection. The M83 $J = 1$ detection is only 1.7σ in LiF1, but it is confirmed in the LiF2 spectrum, so we count it as a detection. For all the other galaxies we only measured upper limits.

For the galaxies in which we detected H_2 absorption, we measured the equivalent widths of the strongest lines and transformed these to H_2 column densities, assuming the absorption is optically thin. For the other galaxies we measured the noise in the spectrum at the expected location of H_2 absorption, and used this to compute 3σ upper limits on the amount of H_2 present. All measurements were made on the LiF1 spectrum because it is the most sensitive. The measured equivalent widths of the strongest lines and the derived H_2 column densities or upper limits are given in Table 3. A model H_2 spectrum was created using the column densities for each J level listed in Table 3 and assuming a Doppler broadening parameter of $b = 15$ km s^{-1}. The model is shown as the smooth black line in Figure 6.

The upper limits on the total H_2 column density are also shown in Table 3. These were derived by simply summing the measured upper limits (or detections) in the $J = 0-4$ levels. In typical Milky Way ISM conditions most ($> 90\%$) of the H_2 is in the $J = 0$ and $J = 1$ states (*e.g.*, Snow et al. 2000, Friedman et al. 2000, Sembach et al. 2001). If this is true in the starbursts as well, the upper J levels should not contribute much to the total H_2 column density. However, since the conditions in the ISM of the starbursts may be different (*e.g.*, the potentially stronger UV radiation field could populate the higher J levels), summing all five levels may be appropriate.

Table 4 lists an estimate of the upper limits on the mass of H_2 detectable by *FUSE* within the aperture. It is important to note that this does not correspond to the total H_2 mass in the aperture, because the majority of the molecular gas is too dense to be detected by *FUSE* (see section 5.1). To determine this limit we first applied the measured column density upper limit to the entire aperture, or in other words we assumed the entire aperture is filled with H_2 at the column density listed in Table 3. The angular area of the aperture was converted to linear area at the assumed distance of the galaxy (see Table 1), and multiplied by the column density limit. As we discuss in detail below, these upper limits need to be treated carefully, given the strong bias in these far-UV spectra against the dustiest lines-of-sight.

TABLE 3. DIFFUSE H_2 CONTENT OF THE SAMPLE GALAXIES[a]

Line ID	Wavelength (Å)	Equivalent Width (mÅ)	N(H_2) (10^{14} cm^{-2})
NGC 1705			
8-0 R(0)	1001.83	< 23.0	< 0.97
7-0 R(1)	1013.44	< 12.2	< 0.66
7-0 R(2)	1014.98	< 14.6	< 0.85
7-0 R(3)	1017.43	< 11.9	< 0.72
5-0 R(4)	1044.54	< 10.2	< 0.70
total[b]			< 3.90
NGC 3310			
4-0 R(0)	1049.37	< 15.6	< 0.69
8-0 R(1)	1002.46	< 22.5	< 1.38
7-0 R(2)	1014.98	< 15.9	< 0.92
4-0 R(3)	1053.98	< 17.1	< 1.34
total[b]			< 4.33
NGC 4214			
8-0 R(0)	1001.83	< 29.4	< 1.24
8-0 R(1)	1002.46	< 41.4	< 2.54
7-0 R(2)	1014.98	< 22.8	< 1.32
7-0 R(3)	1017.43	< 29.1	< 1.76
5-0 R(4)	1044.54	< 19.2	< 1.33
total[b]			< 8.19
M83			
8-0 R(0)	1001.83	< 22.11	< 0.93
9-0 R(1)	992.018	25.6 ± 15.0	1.62 ± 0.95
7-0 R(2)	1014.98	< 22.9	< 1.30
9-0 R(3)	995.974	< 29.1	< 1.90
6-0 R(4)	1032.35	< 35.7	< 2.20
total[b]			< 8.90
NGC 5253			
4-0 R(0)	1001.83	< 24.9	< 1.22
8-0 R(1)	1002.46	70.3 ± 12.5	4.36 ± 0.56
4-0 R(2)	1051.51	24.2 ± 8.6	1.77 ± 0.63
8-0 R(3)	1006.42	< 26.1	< 1.80
5-0 R(4)	1044.54	< 19.2	< 1.30
total[b]			< 11.64

[a]Upper limits are 3σ.
[b]The upper limit on the total H_2 column density detected in the *FUSE* spectra, derived by summing the $J = 0-4$ levels.

The upper limits in Table 3 do not account for the possible presence of unresolved, saturated absorption. Cold H_2 clouds with $T = 100$ K may have Doppler b-values $\lesssim 1$ km s^{-1}. A saturated absorption line with a b-value of 1 km s^{-1} will have an equivalent width $EW \lesssim 10$ mÅ. Such a line could easily go undetected in the *FUSE* data presented here, given the typical upper limits listed in Table 3. Typical b-values measured for H_2 in the Milky Way and Magellanic Clouds are much broader than this, ranging from 2.3 to 20 km s^{-1} (see Shull et al. 2000, Tumlinson et al. 2002). This broadening is most likely due to bulk motions within individual clouds and the velocity dispersion of the ensemble of clouds. If $b = 3$ km s^{-1}, $EW \gtrsim 17$ mÅ, which would result in a 2σ detection in most cases. If unresolved, saturated absorption is present it would result in the underestimation of the upper limits on the H_2 column density.

4.2. *Atomic Hydrogen*

Table 4 shows an estimate of (or lower limit on) the H I column density in the *FUSE* aperture. The H I column was estimated in different ways for each galaxy. Heckman et al. (2001a) derived the H I abundance in NGC 1705 by fitting the Lyβ and higher order H I lines in the *FUSE* spectrum. For NGC 3310, NGC 4124, and NGC 5253 we measured the equivalent width of the Ar I 1066.660 Å line and con-

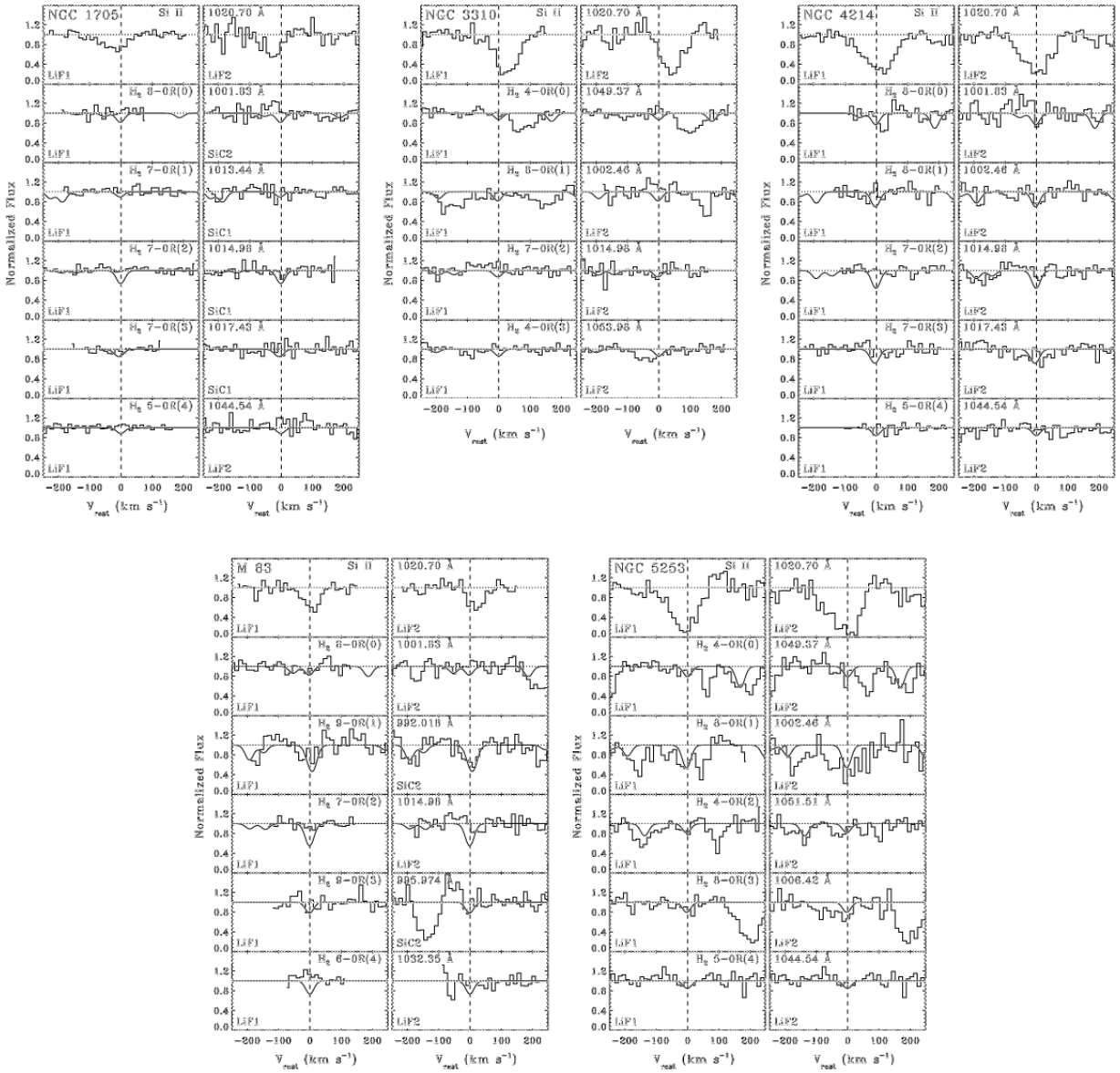

FIG. 6.— Interstellar absorption line profiles from the *FUSE* spectra of the five starburst galaxies. The histogram is the observed spectrum, and the smooth line is a model H_2 spectrum based on the column densities listed in Table 3. For each galaxy we show the Si II 1020.699 Å profile and the expected locations of H_2 lines from rotational levels $J = 0-4$ (except NGC 3310, for which no suitable $J = 4$ line was found). Two channels are shown for each line, although the measurements were made on the channel with the highest S/N (LiF1). The velocity scale has been set so that absorption intrinsic to the galaxy falls at 0 km s^{-1}, using the velocities listed in Table 1.

verted this to a column density assuming the line is optically thin. The Ar I column density was converted to H I by assuming the relative Warm Neutral Medium abundances given by Sembach et al. (2000), and scaling down by the O/H value given in Table 1. This line was used because dust depletion is not important for Ar I (e.g. Aloisi et al. 2003). It is also a relatively weak line, so while the assumption that it is optically thin is likely invalid for most of these galaxies, it gives a better lower limit to the column density than would a stronger line. However, there can be a significant ionization correction for Ar I, and furthermore the O/H values in H II regions (used here) are usually higher than those in the neutral ISM (see *e.g.*, Thuan et al. 2002; Aloisi et al. 2003). Thus, this approach gives a conservative lower limit to N(H I) for most of these sight lines. The Ar I line was not detected in the *FUSE* spectrum of M83, so we measured the O I 950.885 Å line, and converted this to H I using the O/H value given in Table 1. This value is almost identical to the upper limit on N(H I) derived from the non-detection of the Ar I line, so we treat it as an estimate of the H I column density probed by the *FUSE* spectrum, not a lower limit. As we will show in section 5.2, there are indications that the H I column densities are actually much larger than the conservative limits derived above.

The third column in Table 4 lists the molecular hydrogen fractions $f(H_2)$ for the diffuse ISM in each galaxy, defined as:

$$f(H_2) = \frac{2N(H_2)}{[2N(H_2)+N(HI)]}. \quad (1)$$

Since $N(H_2)$ is an upper limit and N(H I) is a lower limit (for three of the galaxies), this expression gives an upper limit to $f(H_2)$. The fact the we are almost certainly underestimating N(H I) implies that the true values of $f(H_2)$ could be as low as

TABLE 4. DIFFUSE H_2 PARAMETERS OF THE SAMPLE GALAXIES

Galaxy	N(H I)[a]	$f(H_2)$[b]	M(H_2)[c] ($M_\odot$)	M(H_2) from CO[d] ($M_\odot$)	I_{1000}[e] (erg s^{-1} cm^{-2} Å^{-1} arcsec^{-2})
NGC 1705	1.6×10^{20}	$< 4.9 \times 10^{-6}$	< 3.5	···	5.6×10^{-16}
NGC 3310	$> 3.0 \times 10^{19}$	$< 2.9 \times 10^{-5}$	< 30.8	$\sim 10^8$	2.0×10^{-16}
NGC 4214	$> 2.7 \times 10^{20}$	$< 6.1 \times 10^{-6}$	< 2.4	$\sim 8 \times 10^5$	1.3×10^{-16}
M83 (NGC 5236)	1.1×10^{19}	$< 1.6 \times 10^{-4}$	< 6.1	$\sim 10^7$	1.9×10^{-16}
NGC 5253	$> 3.0 \times 10^{20}$	$< 7.8 \times 10^{-6}$	< 0.4	$\sim 10^5$	9.0×10^{-16}

[a]H I was determined by converting O I or Ar I absorption measurements in the *FUSE* spectrum (assuming H II region abundances), except for NGC 1705 for which a measurement was available (Heckman et al. 2001a)

[b]The H_2 fraction (see equation 1 in section 4) in the *FUSE* aperture, using the upper limit on total $N(H_2)$ from Table 3. These upper limits refer to the integrated light in the *FUSE* aperture. There are undoubtedly regions within the aperture that have higher molecular fractions.

[c]The upper limit on the total mass of H_2 in the *FUSE* aperture, using the upper limit on total $N(H_2)$ from Table 3. This is only the mass of H_2 detectable with *FUSE*; most of these galaxies contain much more mass in the form of dense clouds which are invisible to *FUSE* (see text).

[d]An estimate of the H_2 mass within the *FUSE* aperture inferred from CO measurements. See section 3 for references.

[e]The measured surface brightness (flux divided by aperture angular area).

10^{-7}, and perhaps even lower if $N(H_2)$ is much below the upper limits in Table 3. However, it is important to note that this upper limit applies to the integrated light in the FUSE aperture, and that there certainly are regions within the aperture, such as the molecular clouds seen in CO emission, in which the molecular fraction is higher.

5. DISCUSSION

5.1. *H_2 in the Dense ISM*

The *FUSE* spectra show very little absorption from H_2 in the starburst regions of these galaxies, with the upper limits on H_2 masses ranging from ~ 31 to < 1 $M_\odot$ (see Table 4). Similar results were found in *FUSE* data for the metal-poor starburst galaxy I Zw 18 (Aloisi et al. 2003; Vidal-Madjar et al. 2000) and for the blue compact dwarf galaxy Mrk 59 (Thuan et al. 2002). This is in stark contrast with CO observations of starbursts, which often reveal large concentrations of molecular gas in the starburst region. Published CO studies of four of the five starbursts in our sample have found many orders of magnitude more H_2 in these galaxies than the *FUSE* measurements imply (see Table 4 and section 3).

The explanation for the difference between the emission and absorption results is that the absorption spectra are not sensitive to the dense clouds seen in CO emission. The combined effects of extinction and the fact that the continuum source is extended biases the far-UV observations toward the least dusty environments, because dust quickly extinguishes the far-UV light in other regions (see *e.g.* Bluhm et al. 2003). Since the most efficient formation mechanism for H_2 is formation on dust grains (Hollenbach & Salpeter 1971), molecular gas is likely concentrated in the dustiest regions. Dense molecular clouds have many magnitudes of extinction in the far-UV, rendering them opaque to the background continuum light. Since large amounts of CO are detected in these galaxies, the lack of H_2 seen in absorption implies that most of the molecular gas is in the form of dense clouds. The continuum that is visible in the *FUSE* spectra passes through the diffuse ISM between the clouds. Since the *FUSE* spectra detect far-UV continuum from these starbursts, the covering factor of the dense molecular clouds in front of the UV continuum source must be < 1.

Although it is tempting to consider the metallicity dependence of the CO–H_2 conversion factor as the cause of the discrepancy between the emission and absorption results, the magnitude of this effect is not nearly large enough to account for the observed difference. Wilson (1995) found a factor of 4.6 increase in the conversion factor for a factor of 10 decrease in metallicity. The metallicity range of the sample is within a factor of 10 from solar abundances, so the discrepancy between the *FUSE* and CO measurements is therefore much too large to be caused by metallicity. Furthermore, metal-poor galaxies such as NGC 5253 should have *more* H_2 than the CO measurements imply, which is the opposite of what we observe.

5.2. *H_2 in the Diffuse ISM*

Sight lines with diffuse H_2 column densities ranging from $10^{14} - 10^{21}$ cm^{-2} are ubiquitous in the Milky Way and Magellanic Clouds (Savage et al. 1977; Shull et al. 2000; Tumlinson et al. 2002). Indeed, it is difficult to find a sight line that extends more than ~ 1 kpc that does not show absorption from H_2. Absorption from H_2 has also been detected in *FUSE* spectra of H II regions in M33 (Bluhm et al. 2003). It is thus surprising to see so little H_2 absorption in the starburst spectra. In this section we discuss how observational biases may explain the results, but also give evidence arguing that the lack of H_2 absorption in the *FUSE* spectra points to a real difference in the diffuse ISM in starbursts.

5.2.1. *Observational Selection Effects*

It is possible that the biases discussed in the previous section also prevent us from detecting H_2 in the diffuse ISM. Simply put, if the spatially extended continuum source (the starburst) is thought of as many individual sight lines within the aperture, then those sight lines with the least extinction (and therefore the lowest H_2 column density) will contribute the most to the composite continuum. *Copernicus* observations of sight lines to hot stars in the Milky Way show a pronounced increase in the molecular hydrogen column density occurring at $E(B-V) = 0.08$, corresponding to $N(H_2) = 10^{19}$ cm^{-2} (Savage et al. 1977; also see Figure 7). Bohlin, Savage, & Drake (1978) showed that the amount of total hydrogen (H I+H_2) that corresponds to this amount of reddening ($\sim 5 \times 10^{20}$ cm^{-2}) is enough to shield H_2 from destruction by UV photons, explaining the marked increase in column density. If the continuum at 1000 Å is dominated by sight lines with $E(B-V) < 0.08$, it is possible that we would

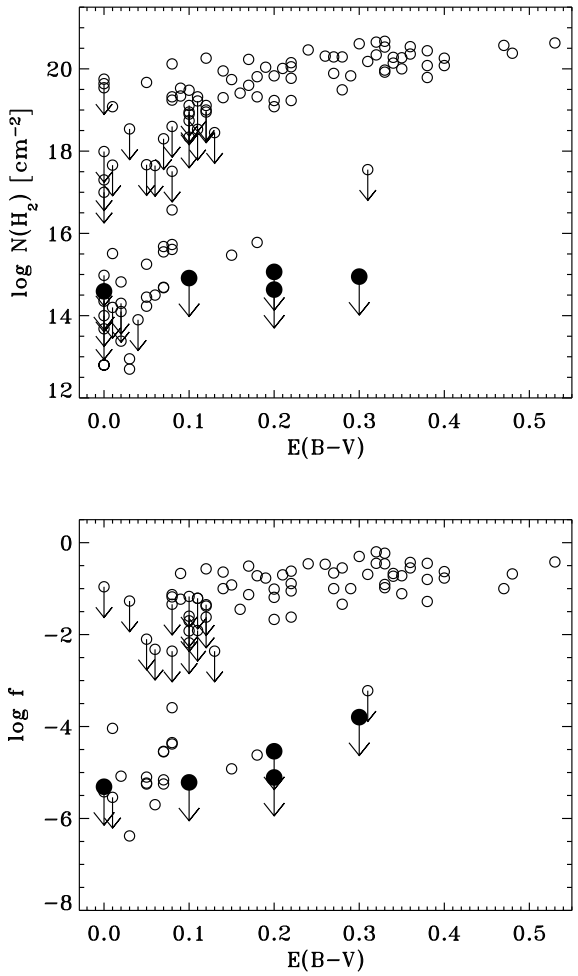

FIG. 7.— The H_2 column density (top panel) and molecular fraction f (bottom panel) versus reddening. The solid symbols are the *FUSE* starburst upper limits, and the open symbols are *Copernicus* measurements and limits for Galactic sight lines (from Savage et al. 1977). The H_2 column densities and molecular fractions in the starbursts are lower than the Galactic sight lines for similar reddenings (except for NGC 1705). Note that the molecular fractions for the starbursts are probably much lower than the derived upper limits due to the probable underestimation of the HI column density. The three highly-reddened Galactic sight lines marked with double circles were noted by Savage et al. (1977) as possibly having strong radiation fields.

not see any H_2 absorption since these sight lines are the least likely to contain H_2. Indeed, if the lower limits on the H I column densities in Table 4 are close to the true values, they would suggest that the sight lines probed by the *FUSE* spectra lack the shielding necessary for the survival of H_2. The *FUSE* data by themselves seem consistent with the *Copernicus* results for the Galaxy.

5.2.2. *Arguments for a Deficiency of Diffuse H_2*

Because the lower limits on N(H I) given in Table 4 are based on lines that are very likely saturated, they may severely underestimate the true column density. Given this limitation, it may be more useful to compare the average *reddening* in the starburst sight lines with the Milky Way. Spectra of these starbursts taken with the *International Ultraviolet Explorer (IUE)* and *Hopkins Ultraviolet Telescope (HUT)* show that the reddening within these galaxies is substantial (Meurer, Heckman, & Calzetti 1999; Leitherer et al. 2002). As listed in Table 1, $E(B-V)$ is $\sim$0 in NGC 1705, but ranges from 0.2 to 0.3 in the other four galaxies. Scaling to the observed metallicities in the starbursts assuming a Milky Way ratio of dust/metals in the ISM, the implied H I column densities range from one to several $\times 10^{21}$ cm^{-2} in these four cases.

While the *FUSE* spectra are certainly biased toward the sight lines with the lowest amount of reddening, it still appears that the majority of sight lines that contribute to the UV flux are reddened by $E(B-V) = 0.2-0.3$ (except for NGC 1705). Now we can directly compare the starburst sight lines with those in the Milky Way. Savage et al. (1977) compared $N(H_2)$ and $E(B-V)$ for Milky Way sight lines. This comparison is reproduced in Figure 7 with the starburst points included. The H_2 column densities and molecular fractions in the starbursts are lower than the Galactic sight lines for similar amounts of reddening (except for NGC 1705). While there is uncertainty in the amount of H I along the sight lines, the reddening values, measured in the UV, are well within the range of H_2 bearing sight lines in the Milky Way. Note that the molecular fractions (f) for the starbursts are probably much lower than the derived upper limits if the measured $E(B-V)$ values are correct and a Milky Way gas/dust ratio is assumed. Thus, the difference between the starbursts and the Milky Way sight lines in Figure 7 may be even more pronounced. Figure 7 suggests that there is a deficiency of H_2 outside of dense clouds in starbursts compared to the Milky Way.

This interpretation is consistent with the lower limits on N(H I) and the measured $E(B-V)$. Indeed, if there is a Milky Way H_2 abundance in the starbursts, there must be a difference between the $E(B-V)$ values in the *IUE* and *FUSE* bands. It is possible to envision scenarios where the actual extinction at 1000 Å is smaller than that measured in the 1200 – 1800 Å spectral range of *IUE*, since the rise in the extinction curve causes the most reddened sight lines to contribute proportionally less to the total flux at shorter wavelengths. However, comparing the entire *HUT* spectrum with reddened model starburst SEDs shows a very good match even in the 1000 – 1200 Å *FUSE* range (see Figure 8), which would not be the case if the spectrum at 1000 Å were preferentially unreddened compared to the longer wavelength data. The generic SEDs in Figure 8 match the data very well even though we did not attempt to match the models to the metallicity or stellar content of the galaxies. This strongly suggests that there is still substantial reddening at 1000 Å, with $E(B-V) = 0.1-0.3$.

Another factor to take into account is the possibility that there is a significant amount of ionized gas along the sight lines. Heckman et al. (2001a) showed that this is true for NGC 1705. Figure 6 shows that the Si II absorption in M83 is much weaker than in the other galaxies (except NGC 1705), implying a lower column of neutral gas. The N(H I) measurement is only $\sim 10^{19}$ cm^{-2}, two orders of magnitude smaller than the H I column implied by the reddening. The discrepancy between the reddening and the neutral gas column may indicate that most of the hydrogen in the diffuse ISM along the sight line is ionized. Studies of sight lines in the Galaxy have shown that the dust content of the ionized ISM is similar to that in the neutral gas (Howk & Savage 1999).

If extinction limited the *FUSE* spectra to only a few nearly unreddened sight lines, the continuum would contain the light of a small number of stars, and they would perhaps only probe the outer edge of the galaxy. This is ruled out by the spectra

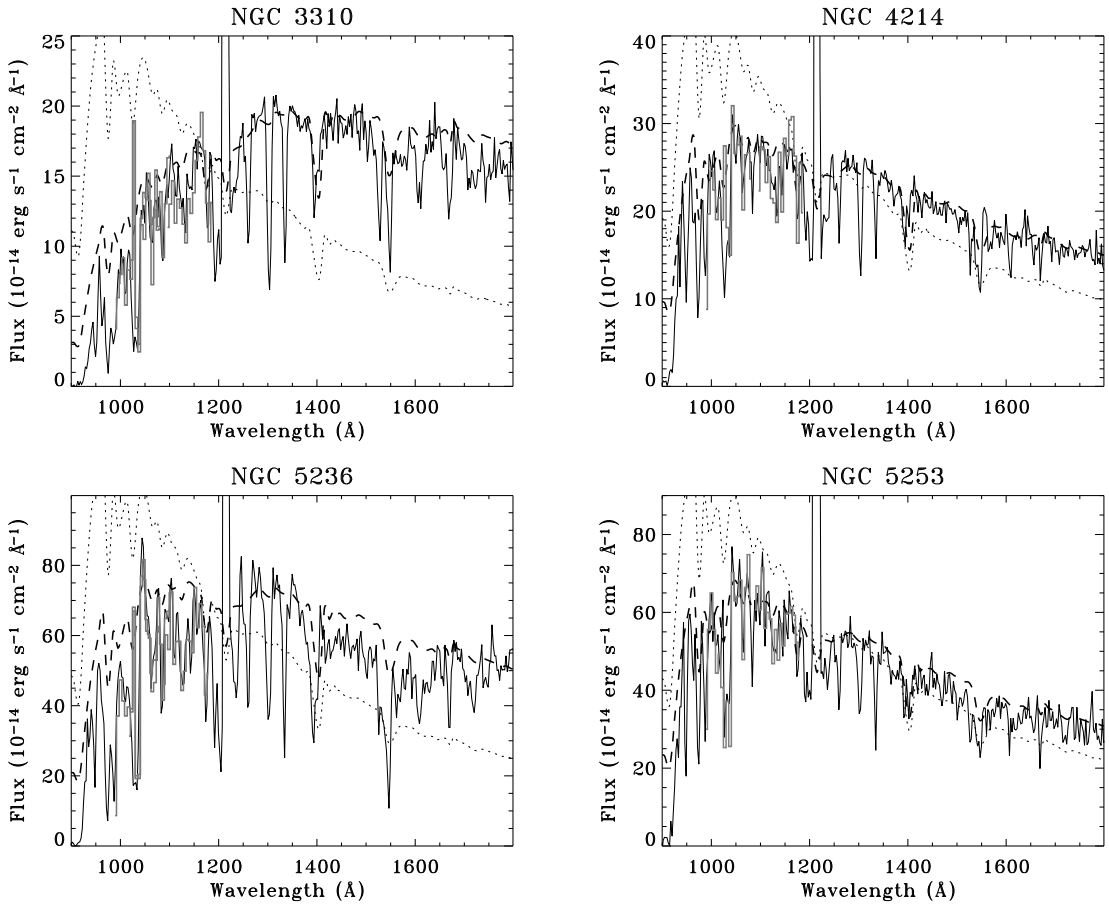

FIG. 8.— The *Hopkins Ultraviolet Telescope (HUT)* spectra of the four most reddened galaxies in our sample (NGC 1705 is excluded). The *FUSE* spectra are also shown as gray thick lines. The dotted line in each panel is the SED of a 100 Myr continuous star formation model, from Starburst99 (Leitherer et al. 1999). The dashed line shows the same SED reddened using the starburst extinction law as given in Leitherer et al. (2002). The reddening values applied were chosen to give the best fit (by eye) to the observed *HUT* spectra, and the resulting $E(B-V)$ values are all within ± 0.1 of those listed in Table 1. The models match the data reasonably well, even near 1000 Å, where the H_2 measurements were made. In some of the panels the attenuation at 1000 Å is underestimated, implying that there is more dust/gas along the sight line than the reddening values in Table 1 would indicate. This figure illustrates that the observed spectra are consistent with $E(B-V)$ values of at least $0.1-0.3$ at 1000 Å, and are not consistent with zero reddening.

themselves. The stellar features seen in the far-UV continuum in all cases is dominated by light from a very young population of O and B stars (e.g. Leitherer et al. 2002; Robert et al. 2003; Leitherer et al. in preparation) and the UV fluxes imply the presence of ~ 1000 such sources (or more if they are reddened). Furthermore, the kinematic signature of the starburst outflow is also clearly evident in the O VI lines (Heckman et al. 2001a,b), which indicates that the continuum source is the starburst, rather than just a few OB stars in the outer halos of the galaxies.

To summarize, the upper limits on $N(H_2)$ derived from the *FUSE* starburst spectra are consistent with the Savage et al. (1977) Milky Way relationship between $N(H_2)$ and $N(H\ I)$ in the diffuse ISM. They cannot rule out, however, a deficiency of $N(H_2)$ compared to Milky Way sight lines with similar amounts of reddening in four of the galaxies. Indeed, when the *IUE* and *HUT* measured reddening is included in the analysis, the data point to such a deficiency. However, with the differences in the *IUE*, *HUT*, and *FUSE* apertures, and the possibility of differences in the reddening measured at *FUSE* versus *IUE* wavelengths, the present data cannot definitively rule out a Milky Way H_2 abundance in the diffuse ISM of these starbursts.

5.3. *Formation and Destruction of H_2*

If the suggested lack of H_2 in the diffuse ISM of starbursts is real, there are implications for H_2 formation and destruction mechanisms. Low column densities of H_2 in the diffuse ISM could be caused by either inhibited formation or rapid destruction of H_2. Tumlinson et al. (2002) and Browning, Tumlinson, & Shull (2003) calculated the effects of a stronger radiation field and a lower H_2 formation rate on $f(H_2)$. To reproduce such low $f(H_2)$ values at the observed H I column densities requires a radiation field at least 50 times stronger than the Galactic mean UV radiation field, or a formation rate less than 1/10th that of the Milky Way, or a combination of both effects (see Figure 4 in Browning et al. 2003).

Inhibited formation is an attractive scenario in metal-poor galaxies because of the deficiency of dust grains on which to form molecules. While the most efficient mechanism for H_2 formation is on the surfaces of dust grains (Hollenbach & Salpeter 1971), other mechanisms have been proposed to occur in the absence of dust (Jenkins & Peimbert 1997). However, the fact that the *FUSE* spectra show no H_2 absorption in galaxies where H_2 is known to exist indicates that the H_2 is associated with dust. This suggests that formation on the surface of grains is the dominant mechanism in

these galaxies.

Vidal-Madjar et al. (2000) and Aloisi et al. (2003) used *FUSE* to search for H_2 absorption in I Zw 18, and Thuan et al. (2002) did the same for Mrk 59. These are both metal-poor galaxies undergoing star formation. They set low upper limits on the abundance of H_2 in the diffuse ISM, similar to those we find for our sample of starbursts. Because I Zw 18 and Mrk 59 have not been detected in CO it is not known whether these galaxies contain any H_2, even in the form of dense clouds. Thus it was not clear to what extent the low metallicity inhibited the formation of molecular gas. Our sample spans a wide range of metallicity, and the CO detections in most of the galaxies in our sample establish that large amounts of molecular gas have formed. This suggests that inhibited formation is not the only factor leading to the low H_2 content in the diffuse ISM. Furthermore, M83 and NGC 3310 have high metal abundances and are very bright far-infrared sources (Calzetti et al. 1995), indicating the presence of dust. Yet we still detect very little H_2 outside of dense molecular clouds, ruling out metallicity as the culprit for those galaxies at least.

The remaining scenario then is rapid destruction. In this scenario molecules of H_2 that evaporate from the surfaces of the dense clouds are photodissociated by UV radiation (Stecher & Williams 1967). The intense UV radiation fields of starburst galaxies may create an environment where the destruction of H_2 would be enhanced. Browning et al. (2003) modeled the formation and destruction of H_2 in the Milky Way and Magellanic Clouds. They assume $I = 1 \times 10^8$ photons cm^{-2} s^{-1} Hz^{-1} for the Galactic radiation field, which corresponds to a surface brightness 1.1×10^{-18} ergs cm^{-2} s^{-1} Å^{-1} arcsec^{-2} at 1000 Å. Table 4 lists the surface brightness at 1000 Å for each galaxy, measured from the *FUSE* spectra by dividing the flux by the angular area of the aperture. All are more than 100 times stronger than the Galactic radiation field, neglecting any possible effects of extinction. This is an average across the aperture, and since the aperture is not uniformly filled with UV continuum the radiation field is undoubtedly stronger at some locations. According to the Browning et al. (2003) models this is more than enough to produce the low $f(H_2)$ values seen in these galaxies, even if there is no reduction in the formation rate. In addition to the effects of UV radiation, the multiple supernovae that have occurred in these galaxies produce fast shocks in the ISM, which can also enhance the dissociation of molecular gas. In such a harsh environment it would not be surprising to find that there is too little H_2 in the diffuse ISM to detect. It is interesting to note that the three highly-reddened Galactic sight lines marked as double circles in Figure 7 (θ^1 Ori C, 29 CMa, 30 CMa) were noted by Savage et al. (1977) for their abnormally low H_2 column densities, possibly due to an unusually strong dissociating radiation field. These sight lines lie the closest to the starbursts in the figure.

5.4. *Dust in the Diffuse ISM*

We have given arguments that there is very little H_2 in the diffuse ISM of these starbursts. We have also shown that the ultraviolet radiation field in these galaxies is strong enough to destroy H_2 in the diffuse ISM. However, as previously discussed, UV spectroscopy has shown that there is substantial reddening of the UV continuum, indicating the presence of dust in the diffuse ISM of these galaxies (except perhaps for NGC 1705, which is close to unreddened). Thus, the molecular gas and dust may have different distributions in these galaxies: H_2 is confined to dense clumps that are highly optically thick to the far-UV continuum, and is absent in the diffuse ISM. However, dust grains exist in both dense and diffuse environments. If the starbursts are deficient in diffuse H_2, the mechanism responsible for dissociating H_2 (UV radiation field, shocks, or both) apparently is not strong enough to destroy all of the dust.

These arguments also support the idea that the covering factor of the dense clumps in front of the UV continuum source is small. Meurer et al. (1999) found an empirical relation between spectral slope β and the ratio of far-infrared (FIR) to UV fluxes, such that galaxies with strong FIR flux relative to UV flux have shallower (redder) UV spectra. The FIR excess can be attributed to dust extinction in the UV, so their conclusion was that starbursts with high extinction are also reddened. This relationship can only exist if the covering factor of dense clumps is small, because these clumps produce FIR flux but do not redden the UV spectrum since they are opaque to UV continuum. The picture based on theoretical modeling of the Meurer et al. (1999) result by Witt & Gordon (2000), Charlot & Fall (2000), and others (see Calzetti 2001 for a recent review) is that the strong correlation between the UV color and the ratio of far-IR to UV flux can only be understood in the context of an inhomogeneous dusty medium lying in the foreground between the UV sources and observer. Our results imply that this medium (which is translucent to far-UV photons) contains substantial amounts of dust but not molecular gas.

NGC 1705 is an interesting case: its UV spectral slope is close to that of an unreddened young stellar population (Meurer et al. 1999), and unlike the other galaxies in our sample it is not a strong far-infrared source (Calzetti et al. 1995). These facts suggest that it contains less dust than the other starbursts in the sample, similar to I Zw 18 and Mrk 59. However, we cannot yet say that these galaxies are devoid of molecular gas. Cannon et al. (2002) used narrow-band imaging to map the dust content of I Zw 18. The dust mass is consistent with the low-metallicity and low FIR emission, and the morphology is very clumpy. If the dense H_2 is traced by dust, this clumpiness would explain the non-detection with *FUSE*. It seems likely that there is molecular gas in I Zw 18, even though it has not been detected in CO emission (perhaps due to low metallicity) or H_2 absorption (due to the clumpy morphology). The same may hold true for NGC 1705 and Mrk 59.

5.5. *Further Implications*

Rigopoulou et al. (2002) carried out a survey of pure rotational emission from H_2 in starbursts (including M83 and NGC 5253) using the *Infrared Space Observatory*. This emission traces warmer H_2 ($T \sim 150$ K) than that typically seen in CO emission ($T \lesssim 100$ K). At least some of the warm gas is thought to be in the photodissociation regions at the surfaces of cold clouds, although there is also evidence for an extended warm component (Valentijn & van der Werf 1999). The survey found that the warm H_2 makes up $1-10\%$ of the total H_2 content derived from CO observations. This is still much higher than the limits on H_2 in the diffuse ISM set with the *FUSE* spectra. Either the column density of an extended warm component is high enough that it is opaque to far-UV light, or the bulk of the warm gas is associated with the dense clouds of cold H_2, suggesting perhaps that is in photodissociation regions.

The low limits on $f(H_2)$ found for these starbursts are remi-

niscent of the values or upper limits measured in damped Lyα systems (DLAs) in QSO spectra (see *e. g.*, Levshakov et al. 2002 and references therein). The difference is that in the starbursts we know there is much more H_2 than is apparent in the *FUSE* spectra, indicating that the spectra are not sensitive to regions in the aperture containing dense H_2. A similar effect may hinder the detection of DLAs with H_2 if the dust associated with the H_2 in such DLAs makes the QSOs behind them invisible (*e.g.*, Fall & Pei 1993). The known QSOs would then preferentially probe DLAs with little extinction, and thus little molecular gas, or systems where the line of sight to the QSO happens to pass through a hole in a clumpy or filamentary H_2/dust distribution (Hirashita et al. 2003). Ellison et al. (2001) found that the underestimate of the population of DLAs due to dust is at most a factor of 2. However, the DLAs that are missed are those with the most H_2 in the line of sight. This would result in an underestimate of the typical H_2 content of DLAs.

6. CONCLUSIONS

We have searched for absorption from H_2 associated with the diffuse ISM in *FUSE* spectra of five starburst galaxies. We have tentatively detected H_2 in M83 and NGC 5253, and set upper limits for NGC 1705, NGC 4214, and NGC 3310. In general there is much less H_2 seen in the far-UV than implied by previous mm-wave CO measurements, as expected if most of the H_2 is in dense clumps which *FUSE* cannot detect because they are opaque to far-UV light. The upper limits on $N(H_2)$ and the lower limits on $N(\mathrm{H\ I})$ in the starbursts are consistent with the Savage et al. (1977) values for the diffuse ISM in the Milky Way. However, the substantial reddening measured in *IUE* spectra of four of the starbursts suggests that the amount of H_2 in the diffuse ISM is much lower than for sight lines in the Milky Way or Magellanic Clouds with similar amounts of reddening. If the suggested deficiency of diffuse H_2 is real, it is likely due to photodissociation of H_2 molecules by UV radiation from massive stars or shocks from multiple supernovae, and illustrates how the harsh environment in starbursts affects the ISM. However, the mechanism that dissociates the molecular gas apparently does not destroy the dust which reddens the UV spectra. The *FUSE* observations show that the absence of H_2 absorption in the far-UV does not necessarily indicate a lack of molecular gas in an actively star-forming galaxy.

We thank the anonymous referee for useful, constructive comments. This work benefited from discussions with Lynn Hacker, B-G Andersson, Bill Blair, Paul Feldman, and Stephen McCandliss. This research has made use of the NASA/IPAC Extragalactic Database (NED) which is operated by the Jet Propulsion Laboratory, California Institute of Technology, under contract with the National Aeronautics and Space Administration. This project was supported by NASA grant NAG5-9012.

REFERENCES

Aloisi, A., Savaglio, S., Heckman, T. M., Hoopes, C. G., Leitherer, C., & Sembach, K. R. 2003, ApJ, 595, 760
Balick, B. & Heckman, T. 1981, A&A, 96, 271
Bluhm, H., de Boer, K. S., Marggraf, O., Richter, P., & Wakker, B. P. 2003, A&A, 398, 983
Bohlin, R. C., Savage, B. D., & Drake, J. F. 1978, ApJ, 224, 132
Browning, M. K., Tumlinson, J., & Shull, J. M. 2003, ApJ, 582, 810
Calzetti, D. 2001, PASP, 113, 1449
Calzetti, D., Bohlin, R. C., Kinney, A. L., Storchi-Bergmann, T., & Heckman, T. M. 1995, ApJ, 443, 136
Cannon, J. M., Skillman, E. D., Garnett, D. R., & Dufour, R. J. 2002, ApJ, 565, 931
Charlot, S., & Fall, S.M. 2000, ApJ, 539, 718
Conselice, C. J., Gallagher, J. S., Calzetti, D., Homeier, N., & Kinney, A. 2000, AJ, 119, 79
de Vaucouleurs G., de Vaucouleurs, A., Corwin, Jr., H., Buta, R., Paturel, F., & Fouqué, P. 1991, Third Reference Catalogue of Bright Galaxies (RC3)
Dixon, W. V. D., Hurwitz, M., & Bowyer, S. 1998, ApJ, 492, 569
Ellison, S. L., Yan, L., Hook, I. M., Pettini, M., Wall, J. V., & Shaver, P. 2001, A&A, 379, 393
Fall, S. M. & Pei, Y. C. 1993, ApJ, 402, 479
Friedman, S. D., et al. 2000, ApJ, 538, L39
Gibson, B. K. et al. 2000, ApJ, 529, 723
Gondhalekar, P. M., Johansson, L. E. B., Brosch, N., Glass, I. S., & Brinks, E. 1998, A&A, 335, 152
Greve, A., Becker, R., Johansson, L. E. B., & McKeith, C. D. 1996, A&A, 312, 391
Harris, J., Calzetti, D., Gallagher, J. S., Conselice, C. J., & Smith, D. A. 2001, AJ, 122, 3046
Heckman, T. M., Robert, C., Leitherer, C., Garnett, D. R., & van der Rydt, F. 1998, ApJ, 503, 646
Heckman, T. M., Sembach, K. R., Meurer, G. R., Strickland, D. K., Martin, C. L., Calzetti, D., & Leitherer, C. 2001a, ApJ, 554, 1021
Heckman, T. M., Sembach, K. R., Meurer, G. R., Leitherer, C., Calzetti, D., & Martin, C. L. 2001b, ApJ, 558, 56
Hirashita, H., Ferrara, A., Wada, K., & Richter, P. 2003, MNRAS, 341, L18
Hollenbach, D. & Salpeter, E. E. 1971, ApJ, 163, 155
Howk, J. C. & Savage, B. D. 1999, ApJ, 517, 746
Israel, F. P. & Baas, F. 2001, A&A, 371, 433
Jenkins, E. B. & Peimbert, A. 1997, ApJ, 477, 265
Kikumoto, T., Taniguchi, Y., Suzuki, M., & Tomisaka, K. 1993, AJ, 106, 466
Kinney, A. L., et al. 1993, ApJS, 86, 5
Leitherer, C., et al. 1999, ApJS, 123, 3
Leitherer, C., Li, I.-H., Calzetti, D., & Heckman, T. M. 2002, ApJS, 140, 303
Leitherer, C., Vacca, W. D., Conti, P. S., Filippenko, A. V., Robert, C., & Sargent, W. L. W. 1996, ApJ, 465, 717
Levshakov, S. A., Dessauges-Zavadsky, M., D'Odorico, S., & Molaro, P. 2002, ApJ, 565, 696
Maíz-Apellániz, J., Cieza, L., & MacKenty, J. W. 2002, AJ, 123, 1307
Meier, D. S., Turner, J. L., & Beck, S. C. 2002, AJ, 124, 877
Meurer, G. R., Freeman, K. C., Dopita, M. A., & Cacciari, C. 1992, AJ, 103, 60
Meurer, G. R., Heckman, T. M., Leitherer, C., Kinney, A., Robert, C., & Garnett, D. R. 1995, AJ, 110, 2665
Meurer, G. R., Heckman, T. M., & Calzetti, D. 1999, ApJ, 521, 64
Moos, H. W., et al. 2000, ApJ, 538, L1
Mulder, P. S., van Driel, W., & Braine, J. 1995, A&A, 300, 687
Rigopoulou, D., Kunze, D., Lutz, D., Genzel, R., & Moorwood, A. F. M. 2002, A&A, 389, 374
Robert, C., Pellerin, A., Aloisi, A., Leitherer, C., Hoopes, C.,& Heckman, T. 2003, ApJS, 144, 21
Sahnow, D. J., et al. 2000, ApJ, 538, L7
Savage, B. D., Drake, J. F., Budich, W., & Bohlin, R. C. 1977, ApJ, 216, 291
Sembach, K. R., Howk, J. C., Ryans, R. S. I., & Keenan, F. P. 2000, ApJ, 528, 310
Sembach, K. R., Howk, J. C., Savage, B. D., & Shull, J. M. 2001, AJ, 121, 992
Shull, J. M. et al. 2000, ApJ, 538, L73
Smith, D. A., et al. 1996, ApJ, 473, L21
Snow, T. P., et al. 2000, ApJ, 538, L65
Stecher, T. P. & Williams, D. A. 1967, ApJ, 149, L29
Storchi-Bergmann, T., Calzetti, D., & Kinney, A. L. 1994, ApJ, 429, 572
Strickland, D. K. & Stevens, I. R. 1999, MNRAS, 306, 43
Thim, F., Tammann, G. A., Saha, A., Dolphin, A., Sandage, A., Tolstoy, E., & Labhardt, L. 2003, ApJ, 590, 256
Thuan, T. X., Lecavelier des Etangs, A., & Izotov, Y. I. 2002, ApJ, 565, 941
Tosi, M., Sabbi, E., Bellazzini, M., Aloisi, A., Greggio, L., Leitherer, C., & Montegriffo, P. 2001, AJ, 122, 1271
Tumlinson, J., et al. 2002, ApJ, 566, 857
Valentijn, E. A. & van der Werf, P. P. 1999, ApJ, 522, L29
Vidal-Madjar, A., et al. 2000, ApJ, 538, L77
Walter, F., Taylor, C. L., Hüttemeister, S., Scoville, N., & McIntyre, V. 2001, AJ, 121, 727
Weiss, A., Neininger, N., Hüttemeister, S., & Klein, U. 2001, A&A, 365, 571
Wilson, C. D. 1995, ApJ, 448, L97
Witt, A., & Gordon, K. 2000, ApJ, 528, 799